



TESS Data Release Notes:

Sector 16, DR22

*Michael M. Fausnaugh, Christopher J. Burke
Kavli Institute for Astrophysics and Space Science, Massachusetts Institute of Technology,
Cambridge, Massachusetts*

*Douglas A. Caldwell
SETI Institute, Mountain View, California*

*Jon M. Jenkins
NASA Ames Research Center, Moffett Field, California*

*Jeffrey C. Smith, Joseph D. Twicken
SETI Institute, Mountain View, California*

*Roland Vanderspek
Kavli Institute for Astrophysics and Space Science, Massachusetts Institute of Technology,
Cambridge, Massachusetts*

*John P. Doty
Noqi Aerospace Ltd, Billerica, Massachusetts*

*Eric B. Ting
Ames Research Center, Moffett Field, California*

*Joel S. Villaseñor
Kavli Institute for Astrophysics and Space Science, Massachusetts Institute of Technology,
Cambridge, Massachusetts*

NASA STI Program ... in Profile

Since its founding, NASA has been dedicated to the advancement of aeronautics and space science. The NASA scientific and technical information (STI) program plays a key part in helping NASA maintain this important role.

The NASA STI program operates under the auspices of the Agency Chief Information Officer. It collects, organizes, provides for archiving, and disseminates NASA's STI. The NASA STI program provides access to the NTRS Registered and its public interface, the NASA Technical Reports Server, thus providing one of the largest collections of aeronautical and space science STI in the world. Results are published in both non-NASA channels and by NASA in the NASA STI Report Series, which includes the following report types:

- **TECHNICAL PUBLICATION.** Reports of completed research or a major significant phase of research that present the results of NASA Programs and include extensive data or theoretical analysis. Includes compilations of significant scientific and technical data and information deemed to be of continuing reference value. NASA counterpart of peer-reviewed formal professional papers but has less stringent limitations on manuscript length and extent of graphic presentations.
- **TECHNICAL MEMORANDUM.** Scientific and technical findings that are preliminary or of specialized interest, e.g., quick release reports, working papers, and bibliographies that contain minimal annotation. Does not contain extensive analysis.
- **CONTRACTOR REPORT.** Scientific and technical findings by NASA-sponsored contractors and grantees.

- **CONFERENCE PUBLICATION.** Collected papers from scientific and technical conferences, symposia, seminars, or other meetings sponsored or co-sponsored by NASA.
- **SPECIAL PUBLICATION.** Scientific, technical, or historical information from NASA programs, projects, and missions, often concerned with subjects having substantial public interest.
- **TECHNICAL TRANSLATION.** English-language translations of foreign scientific and technical material pertinent to NASA's mission.

Specialized services also include organizing and publishing research results, distributing specialized research announcements and feeds, providing information desk and personal search support, and enabling data exchange services.

For more information about the NASA STI program, see the following:

- Access the NASA STI program home page at <http://www.sti.nasa.gov>
- E-mail your question to help@sti.nasa.gov
- Phone the NASA STI Information Desk at 757-864-9658
- Write to:
NASA STI Information Desk
Mail Stop 148
NASA Langley Research Center
Hampton, VA 23681-2199



TESS Data Release Notes: Sector 16, DR22

*Michael M. Fausnaugh, Christopher J. Burke
Kavli Institute for Astrophysics and Space Science, Massachusetts Institute of Technology,
Cambridge, Massachusetts*

*Douglas A. Caldwell
SETI Institute, Mountain View, California*

*Jon M. Jenkins
NASA Ames Research Center, Moffett Field, California*

*Jeffrey C. Smith, Joseph D. Twicken
SETI Institute, Mountain View, California*

*Roland Vanderspek
Kavli Institute for Astrophysics and Space Science, Massachusetts Institute of Technology,
Cambridge, Massachusetts*

*John P. Doty
Noqi Aerospace Ltd, Billerica, Massachusetts*

*Eric B. Ting
Ames Research Center, Moffett Field, California*

*Joel S. Villaseñor
Kavli Institute for Astrophysics and Space Science, Massachusetts Institute of Technology,
Cambridge, Massachusetts*

Acknowledgements

These Data Release Notes provide information on the processing and export of data from the Transiting Exoplanet Survey Satellite (TESS). The data products included in this data release are full frame images (FFIs), target pixel files, light curve files, collateral pixel files, cotrending basis vectors (CBVs), and Data Validation (DV) reports, time series, and associated xml files.

These data products were generated by the TESS Science Processing Operations Center (SPOC, [Jenkins et al., 2016](#)) at NASA Ames Research Center from data collected by the TESS instrument, which is managed by the TESS Payload Operations Center (POC) at Massachusetts Institute of Technology (MIT). The format and content of these data products are documented in the [Science Data Products Description Document \(SDPDD\)](#)¹. The SPOC science algorithms are based heavily on those of the Kepler Mission science pipeline, and are described in the Kepler Data Processing Handbook ([Jenkins, 2017](#)).² The Data Validation algorithms are documented in [Twicken et al. \(2018\)](#) and [Li et al. \(2019\)](#). The [TESS Instrument Handbook](#) ([Vanderspek et al., 2018](#)) contains more information about the TESS instrument design, detector layout, data properties, and mission operations.

The TESS Mission is funded by NASA's Science Mission Directorate.

This report is available in electronic form at
<https://archive.stsci.edu/tess/>

¹<https://archive.stsci.edu/missions/tess/doc/EXP-TESS-ARC-ICD-TM-0014.pdf>

²<https://archive.stsci.edu/kepler/manuals/KSCI-19081-002-KDPH.pdf>

1 Observations

TESS Sector 16 observations include physical orbits 39 and 40 of the spacecraft around the Earth. Data collection was paused for 1.29 days during perigee passage while downloading data. In total, there are 23.38 days of science data collected in Sector 16.

Table 1: Sector 16 Observation times

	UTC	TJD ^a	Cadence #
Orbit 39 start	2019-09-12 03:29:27	1738.64697	368058
Orbit 39 end	2019-09-23 20:31:27	1750.35669	376489
Orbit 40 start	2019-09-25 03:35:27	1751.65113	377421
Orbit 40 end	2019-10-06 19:37:26	1763.31918	385822

^a TJD = TESS JD = JD - 2,457,000.0

The spacecraft was pointing at RA (J2000): 282.4427°; Dec (J2000): 66.1422°; Roll: 79.4699°. Two-minute cadence data were collected for 20,000 targets, and full frame images were collected every 30 minutes. See the TESS project [Sector 16 observation page](#)³ for the coordinates of the spacecraft pointing and center field-of-view of each camera, as well as the detailed target list. Fields-of-view for each camera and the Guest Investigator two-minute target list can be found at the TESS Guest Investigator Office [observations status page](#)⁴.

1.1 Notes on Individual Targets

One bright star ($T_{\text{mag}} \lesssim 1.8$) with a large pixel stamp was not processed in the photometric pipeline. A target pixel file with raw data is provided, but no light curve was produced. The affected TIC ID is 260614141.

Ten target stars (150388950, 159190000, 159190005, 283819432, 334487469, 341873045, 471011825, 1102093577, 2022481918, 2022482049) are blended with comparably bright stars—the contaminating flux for these objects is very large, and the resulting photometry for such targets is expected to be unreliable.

1.2 Spacecraft Pointing and Momentum dumps

As in Sector 14 and Sector 15, the pointing in Sector 16 was set at +85 degrees in ecliptic latitude, so that Camera 2 and Camera 3 straddle the ecliptic pole. Both Camera 1 and Camera 4 were used for guiding during this sector.

The reaction wheel speeds were reset with momentum dumps every 5.83 days—there is only one momentum dump in each orbit. Figure 1 summarizes the pointing performance over the course of the sector based on Fine Pointing telemetry.

³<https://tess.mit.edu/observations/sector-16>

⁴<https://heasarc.gsfc.nasa.gov/docs/tess/status.html>

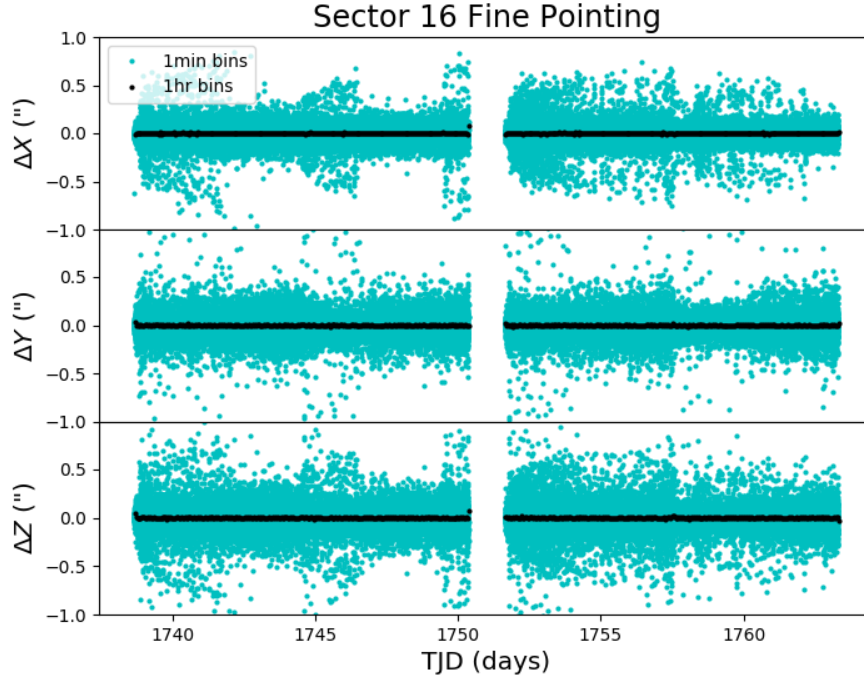


Figure 1: Guiding corrections based on spacecraft fine pointing telemetry. The delta-quaternions from each camera have been converted to spacecraft frame, binned to 1 minute and 1 hour, and averaged across cameras. Long-term trends (such as those caused by differential velocity aberration) have also been removed. The $\Delta X/\Delta Y$ directions represent offsets along the the detectors’ rows/columns, while the ΔZ direction represents spacecraft roll.

1.3 Scattered Light

Figure 2 shows the median value of the background estimate for all targets on a given CCD as a function of time. Figure 3 shows the angle between each camera’s boresight and the Earth or Moon—this figure can be used to identify periods affected by scattered light and the relative contributions of the Earth and Moon to the image backgrounds.

In Sector 16, the Earth is above the sunshade for much of the sector, in a similar way as Sector 14 and Sector 15. The 24 hour rotation period of the Earth and several harmonics thereof are visible as oscillations in the background for most of both orbits.

2 Data Anomaly Flags

See the [SDPDD](#) (§9) for a list of data quality flags and the associated binary values used for TESS data, and the [TESS Instrument Handbook](#) for a more detailed description of each flag.

The following flags were not used in Sector 16: bits 1, 2, 7, 8, 9, and 11 (Attitude Tweak, Safe Mode, Cosmic Ray in Aperture, Manual Exclude, Discontinuity, Cosmic Ray in Collateral Pixel).

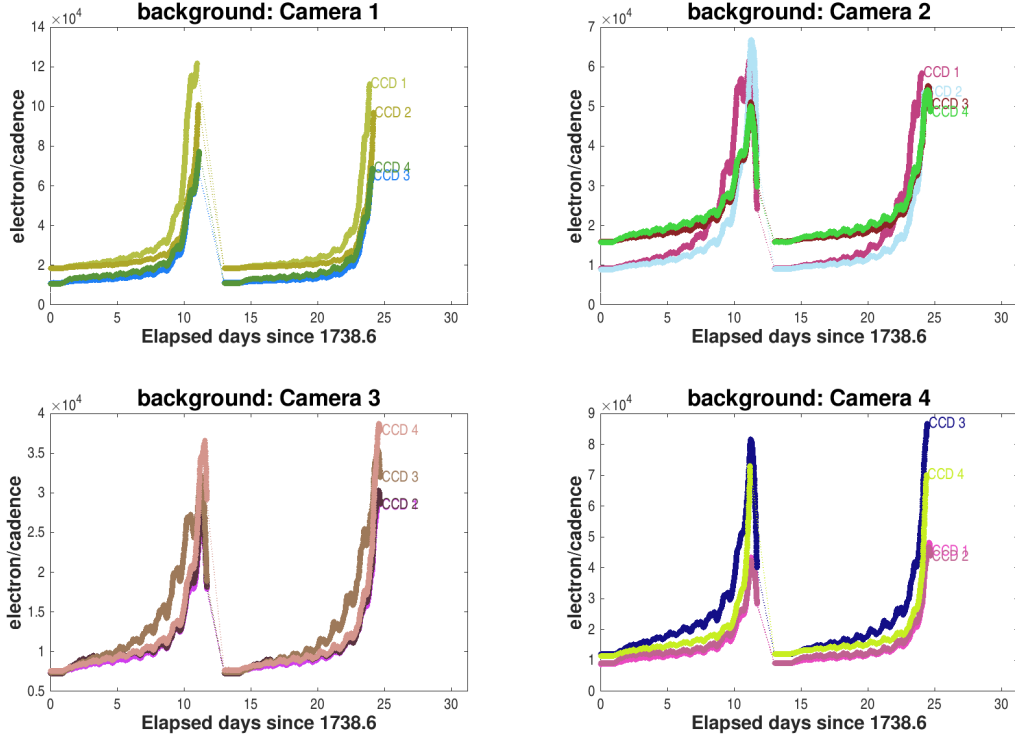


Figure 2: Median background flux across all targets on a given CCD in each camera. The changes are caused by variations in the orientation and distance of the Earth and Moon.

Cadences marked with bits 3, 4, 6, and 12 (Coarse Point, Earth Point, Reaction Wheel Desaturation Event, and Straylight) were marked based on spacecraft telemetry.

Cadences marked with bit 5 and 10 (Argabrightening Events and Impulsive Outlier) were identified by the SPOC pipeline. Bit 5 marks a sudden change in the background measurements. In practice, bit 5 flags are caused by rapidly changing glints and unstable pointing at times near momentum dumps. Bit 10 marks an outlier identified by PDC and omitted from the cotrending procedure.

Cadences marked with bit 8 (Manual Exclude) are ignored by PDC, TPS, and DV for cotrending and transit searches. In Sector 16, these cadences were identified using spacecraft telemetry from the fine pointing system. All cadences with pointing excursions >7 arcseconds (~ 0.3 pixel) were flagged for manual exclude. Note that this is equivalent to our previously reported threshold after accounting for a software bug. However, due to an operational error these flags were not set in the final data processing, and the pointing excursions >7 arcseconds were neither identified with data quality flags in the export products nor ignored by PDC, TPS and DV as desired. The total number of cadences that should have been flagged was only 101. The operational procedure for flagging the Manual Excludes was corrected in Sector 19 (DRN 26).

In Sector 16, bit 13 (value 4096, “Scattered Light”) was set based on the observed background measurements for targets on each CCD, in order to mask cadences that would neg-

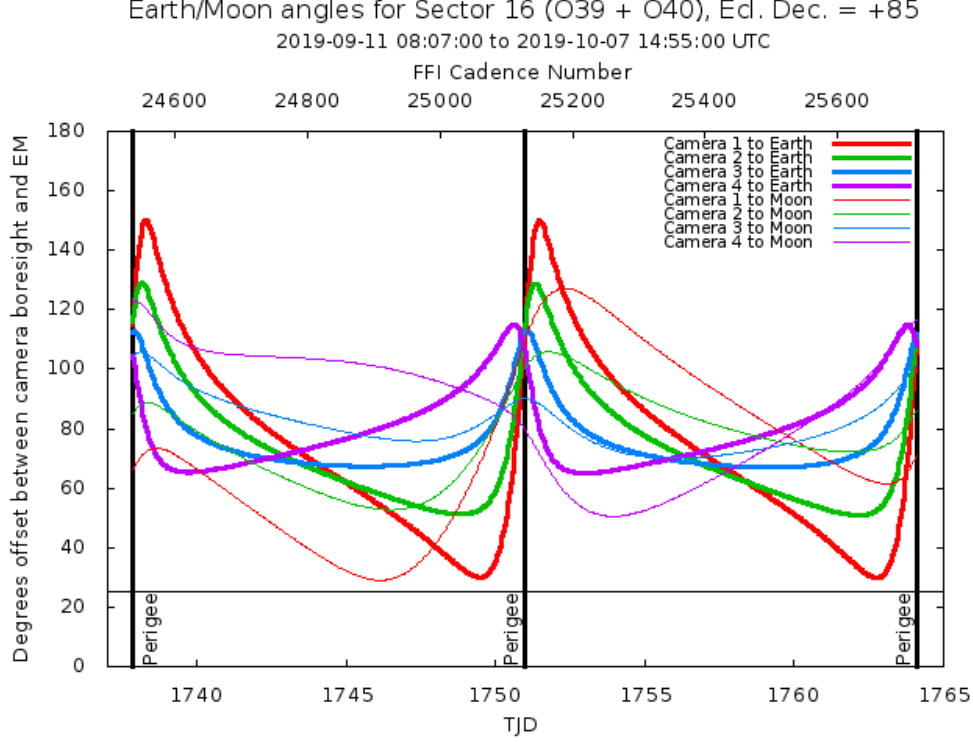


Figure 3: Angle between the four camera boresights and the Earth/Moon as a function of time. When the Earth is within $\sim 25^\circ$ of a camera’s boresight, transiting planet searches may be compromised by high levels of scattered light. At larger angles, up to $\sim 35^\circ$, scattered light patterns and complicated structures may be visible. At yet larger angles, low level patchy features may be visible. Scattered light from the Moon is generally only noticeable below $\sim 35^\circ$. This figure can be used to identify periods affected by scattered light and the relative contributions of the Earth and Moon to the background. However, the background intensity and locations of scattered light features depend on additional factors, such as the Earth/Moon azimuth and distance from the spacecraft.

actively affect the systematic error removal in PDC and the planet search in TPS.

FFIs were only marked with bits 3, 6 and 12 (Course Point, Reaction Wheel Desaturation Events and Straylight). Only one FFI is affected by each momentum dump.

3 Anomalous Effects

3.1 Smear Correction Issues

The following columns were impacted by bright stars in the science frame, and/or upper buffer rows, which bleed into the upper serial register resulting in an overestimated smear correction.

- Camera 4, CCD 2, Column 1986, Star HD 114535
- Camera 4, CCD 3, Column 1465, Star 86 Ursae Majoris

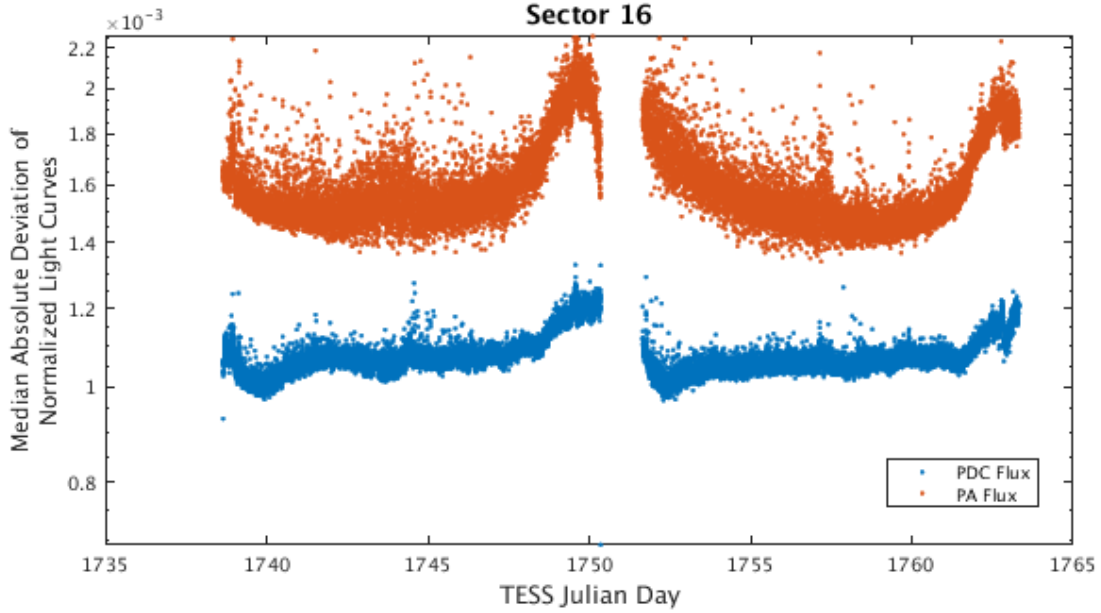


Figure 4: Median absolute deviation (MAD) for the 2-minute cadence data from Sector 16, showing the performance of the cotrending after identifying Manual Exclude data quality flags. The MAD is calculated in each cadence across stars with flux variations less than 1% for both the PA (red) and PDC (blue) light curves, where each light curve is normalized by its median flux value. The scatter in the PA light curves is much higher than that for the PDC light curves, and the outliers in the PA light curves are largely absent from the PDC light curves due to the use of the anomaly flags.

3.2 Fireflies and Fireworks

Table 2 lists all firefly and fireworks events for Sector 16. These phenomena are small, spatially extended, comet-like features in the images—created by sunlit particles in the camera FOV—that may appear one or two at a time (fireflies) or in large groups (fireworks). See the [TESS Instrument Handbook](#) for a more complete description.

Table 2: Sector Fireflies and Fireworks

FFI Start	FFI End	Cameras	Description
2019255032927	2019255035927	2	Firefly
2019268052927	2019268055927	4	Firefly
2019269165927	2019269172927	3	Firefly

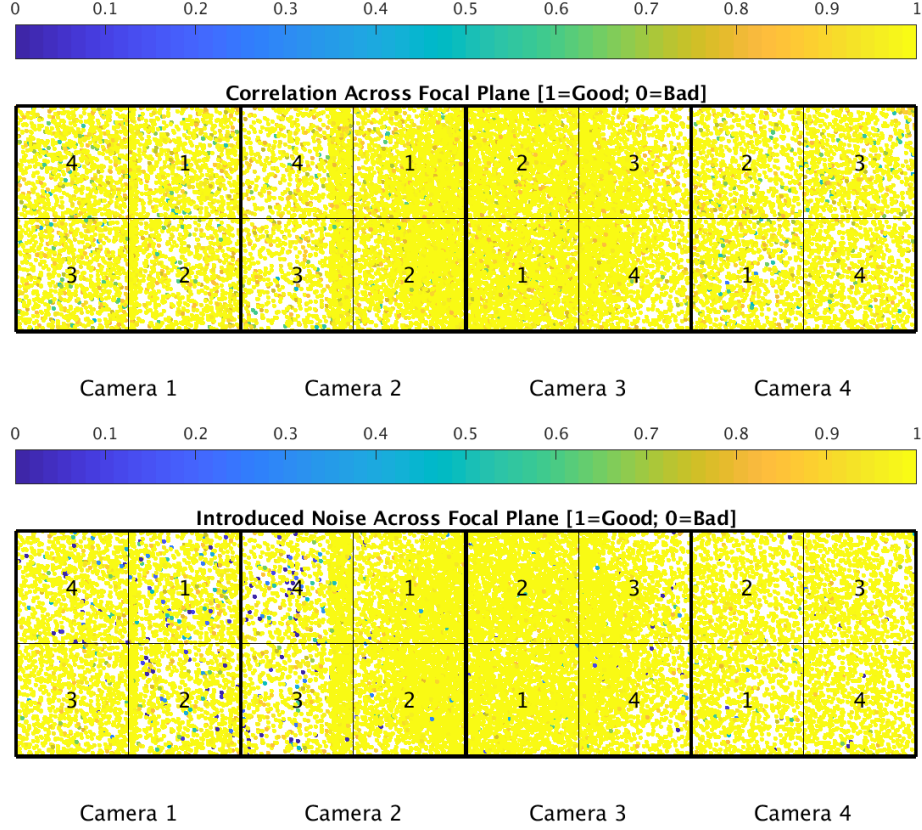


Figure 5: PDC residual correlation goodness metric (top panel) and PDC introduced noise goodness metric (bottom panel). The metric values are shown on a focal plane map indicating the camera and CCD location of each target. The correlation goodness metric is calibrated such that a value greater than 0.8 means there is less than 10% mean absolute correlation between the target under study and all other targets on the CCD. The introduced noise metric is calibrated such that a value greater than 0.8 means the power in broad-band introduced noise is below the level of uncertainties in the flux values.

4 Pipeline Performance and Results

4.1 Light Curves and Photometric Precision

Figure 5 gives the PDC goodness metrics for residual correlation and introduced noise on a scale between 0 (bad) and 1 (good). The performance of PDC is very good and generally uniform over most of the field of view. Figure 6 shows the achieved Combined Differential Photometric Precision (CDPP) at 1-hour timescales for all targets.

4.2 Transit Search and Data Validation

In Sector 16, the light curves of 19999 targets were subjected to the transit search in TPS. Of these, Threshold Crossing Events (TCEs) at the 7.1σ level were generated for 694 targets.

We employed an iterative method when conducting the Sector 16 transit search. The

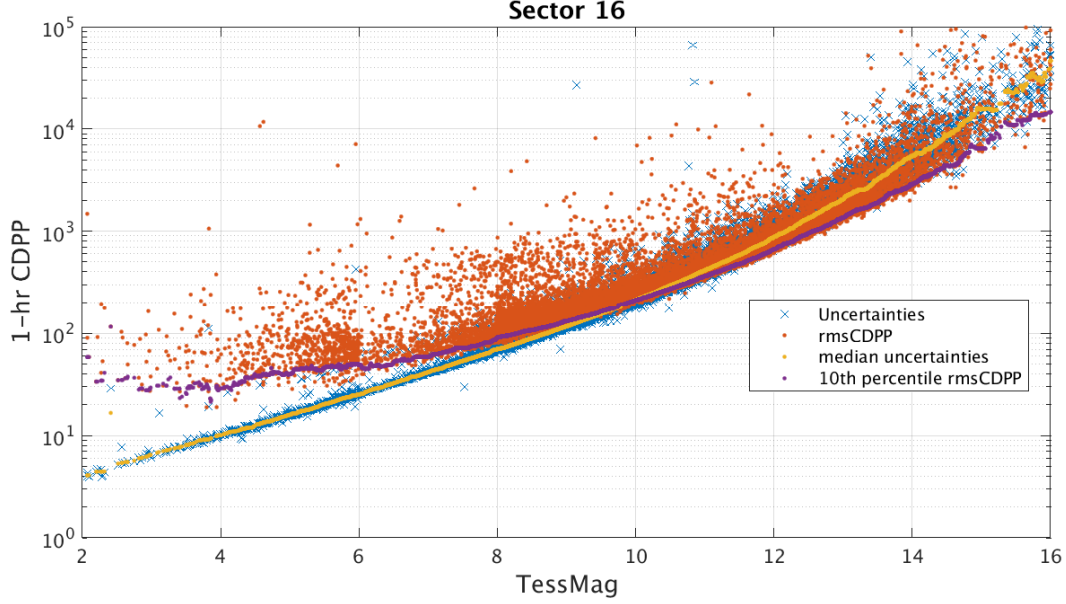


Figure 6: 1-hour CDPP. The red points are the RMS CDPP measurements for the 19999 light curves from Sector 16 plotted as a function of TESS magnitude. The blue x’s are the uncertainties, scaled to 1-hour timescale. The purple curve is a moving 10th percentile of the RMS CDPP measurements, and the gold curve is a moving median of the 1-hr uncertainties.

top panel of Figure 7 shows the number of TCEs at a given cadence that exhibit a transit signal from an initial run of TPS. The 3σ peaks were used to define deemphasis weights for a second run of TPS, the results of which are shown in the bottom panel of Figure 7. The final set of TCEs and the results reported here are based on the second run of TPS. The values of the adopted deemphasis weights are provided in the DV timeseries data products for targets with TCEs.

The top panel of Figure 8 shows the distribution of orbital periods for the final set of TCEs found in Sector 16. The vertical histogram in the right panel of Figure 8 shows the distribution of transit depths derived from limb-darkened transiting planet model fits for TCEs. The model transit depths range down to the order of 100 ppm, but the bulk of the transit depths are considerably larger.

A search for additional TCEs in potential multiple planet systems was conducted in DV through calls to TPS. A total of 1041 TCEs were ultimately identified in the SPOC pipeline on 694 unique target stars. Table 3 provides a breakdown of the number of TCEs by target. Note that targets with large numbers of TCEs are likely to include false positives.

Finally, the difference images in the DV reports have limits applied to the number and magnitude of displayed stars to ensure that the images are not completely covered by labels in crowded regions of the sky. All TIC objects that fall within the axis limits of the centroid offset figures associated with the difference images are marked with TIC ID and Tmag.

Table 3: Sector 16 TCE Numbers

Number of TCEs	Number of Targets	Total TCEs
1	425	425
2	215	430
3	35	105
4	14	56
5	5	25
—	694	1041

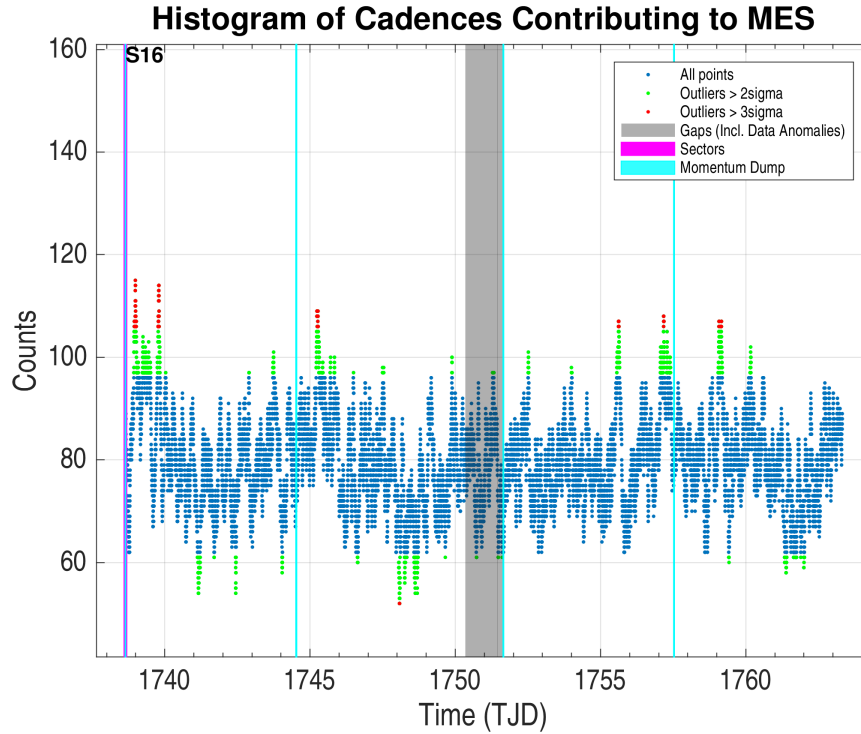
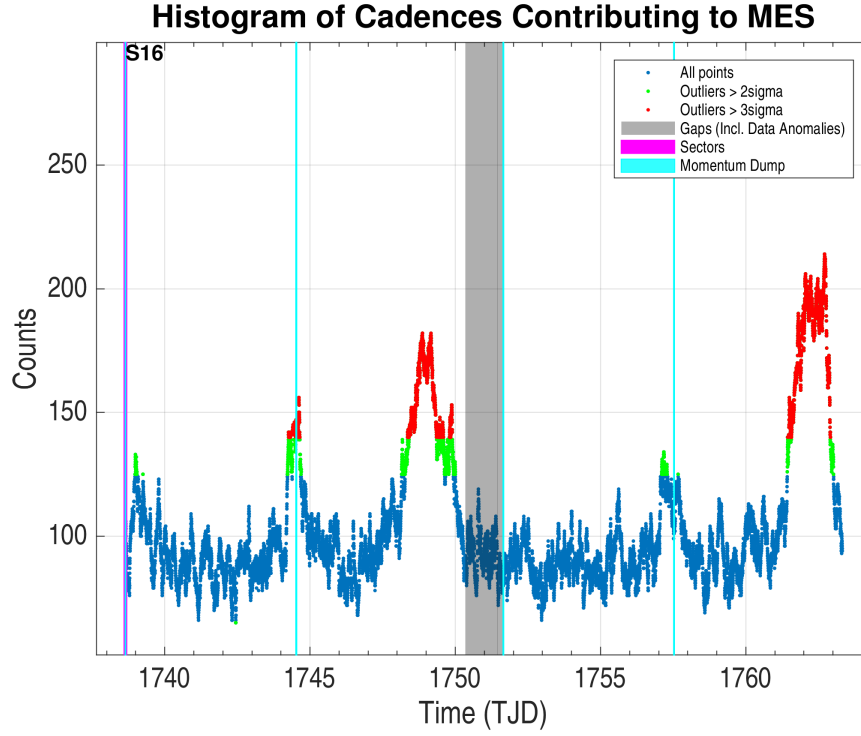


Figure 7: Top panel: Number of TCEs at a given cadence exhibiting a transit signal, based on an initial run of TPS. Any isolated peaks are caused by single events that result in spurious TCEs. These peaks were used to define deemphasis weights that suppress the contribution of problematic epochs to the transit detection statistics in a second iteration of TPS. Bottom panel: Results from the second run of TPS.

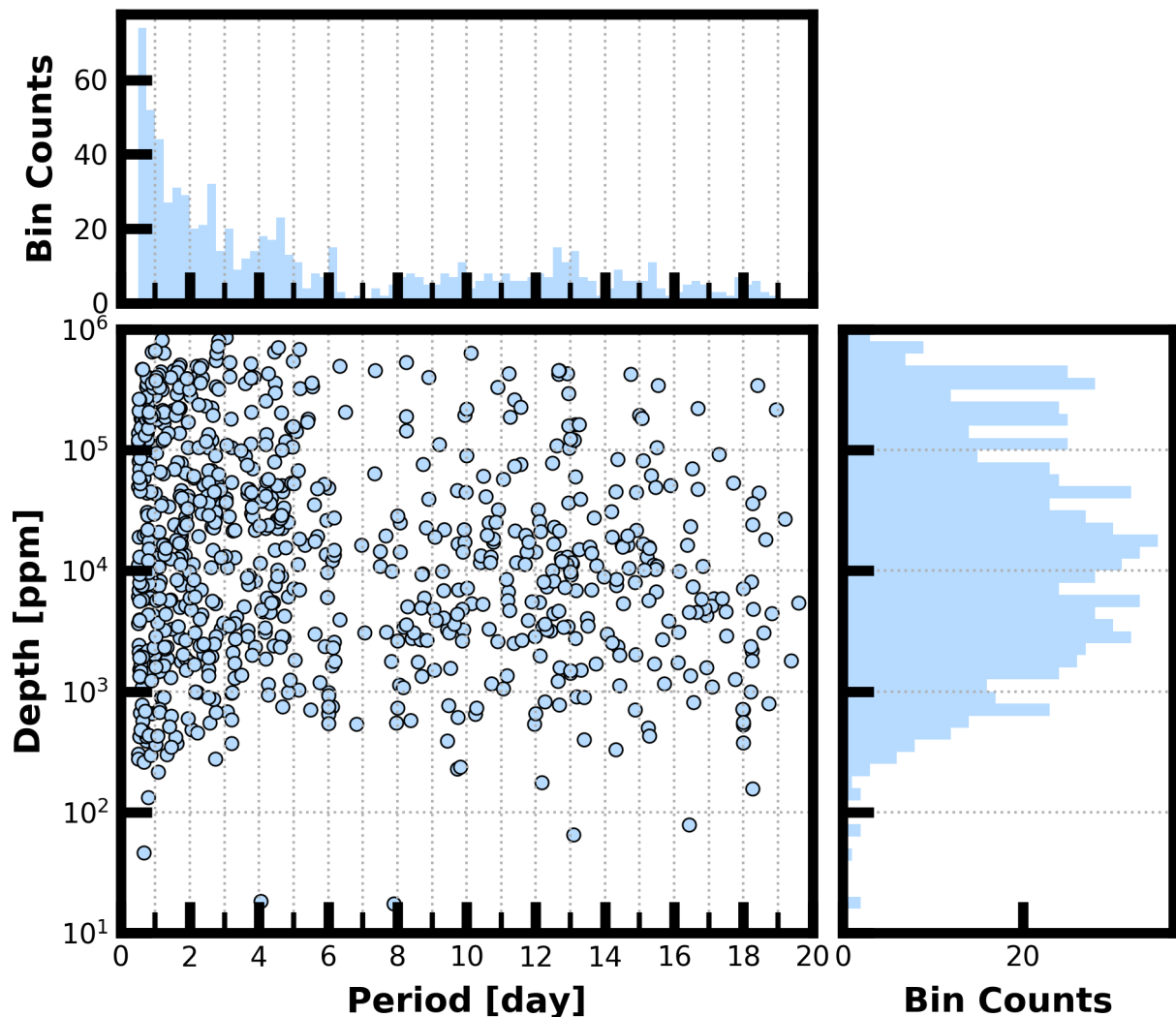


Figure 8: Lower Left Panel: Transit depth as a function of orbital period for the 1041 TCEs identified for the Sector 16 search. For enhanced visibility of long period detections, TCEs with orbital period < 0.5 days are not shown. Reported depth comes from the DV limb darkened transit fit depth when available, and the DV trapezoid model fit depth when not available. Top Panel: Orbital period distribution of the TCEs shown in the lower left panel. Right Panel: Transit depth distribution for the TCEs shown in the lower left panel.

References

- Jenkins, J. M. 2017, [Kepler Data Processing Handbook](#): Overview of the Science Operations Center, Tech. rep., NASA Ames Research Center
- Jenkins, J. M., Twicken, J. D., McCauliff, S., et al. 2016, in Proc. SPIE, Vol. 9913, Software and Cyberinfrastructure for Astronomy IV, [99133E](#)
- Li, J., Tenenbaum, P., Twicken, J. D., et al. 2019, *PASP*, 131, 024506, doi: [10.1088/1538-3873/aaf44d](#)
- Twicken, J. D., Catanzarite, J. H., Clarke, B. D., et al. 2018, *PASP*, 130, 064502, doi: [10.1088/1538-3873/aab694](#)
- Vanderspek, R., Doty, J., Fausnaugh, M., et al. 2018, [TESS Instrument Handbook](#), Tech. rep., Kavli Institute for Astrophysics and Space Science, Massachusetts Institute of Technology

Acronyms and Abbreviation List

BTJD Barycentric-corrected TESS Julian Date

CAL Calibration Pipeline Module

CBV Cotrending Basis Vector

CCD Charge Coupled Device

CDPP Combined Differential Photometric Precision

COA Compute Optimal Aperture Pipeline Module

CSCI Computer Software Configuration Item

CTE Charge Transfer Efficiency

Dec Declination

DR Data Release

DV Data Validation Pipeline Module

DVA Differential Velocity Aberration

FFI Full Frame Image

FIN FFI Index Number

FITS Flexible Image Transport System

FOV Field of View

FPG Focal Plane Geometry model

KDPH Kepler Data Processing Handbook

KIH Kepler Instrument Handbook

KOI Kepler Object of Interest

MAD Median Absolute Deviation

MAP Maximum A Posteriori

MAST Mikulski Archive for Space Telescopes

MES Multiple Event Statistic

NAS NASA Advanced Supercomputing Division

PA Photometric Analysis Pipeline Module

PDC Pre-Search Data Conditioning Pipeline Module

PDC-MAP Pre-Search Data Conditioning Maximum A Posteriori algorithm

PDC-msMAP Pre-Search Data Conditioning Multiscale Maximum A Posteriori algorithm

PDF Portable Document Format

POC Payload Operations Center

POU Propagation of Uncertainties

ppm Parts-per-million

PRF Pixel Response Function

RA Right Ascension

RMS Root Mean Square

SAP Simple Aperture Photometry

SDPDD Science Data Product Description Document

SNR Signal-to-Noise Ratio

SPOC Science Processing Operations Center

SVD Singular Value Decomposition

TCE Threshold Crossing Event

TESS Transiting Exoplanet Survey Satellite

TIC TESS Input Catalog

TIH TESS Instrument Handbook

TJD TESS Julian Date

TOI TESS Object of Interest

TPS Transiting Planet Search Pipeline Module

UTC Coordinated Universal Time

XML Extensible Markup Language